



Published in final edited form as:

Cell. 2014 April 24; 157(3): 565–579. doi:10.1016/j.cell.2014.03.032.

The Oxygen Rich Postnatal Environment Induces Cardiomyocyte Cell Cycle Arrest Through DNA Damage Response

Bao N. Puente^{1,3,*}, Wataru Kimura^{1,*}, Shalini A. Muralidhar¹, Jesung Moon³, James F. Amatruda^{1,2,3}, Kate L. Phelps⁴, David Grinsfelder⁵, Beverly A. Rothermel^{1,2}, Rui Chen¹, Joseph A. Garcia¹, Celio X. Santos⁶, SuWanee Thet¹, Eiichiro Mori¹⁰, Michael T. Kinter⁷, Paul M. Rindler⁷, Serena Zacchigna⁸, Shibani Mukherjee¹⁰, David J. Chen¹⁰, Ahmed I. Mahmoud¹¹, Mauro Giacca⁸, Peter S. Rabinovitch⁹, Asaithamby Aroumougame¹⁰, Ajay M. Shah⁶, Luke I. Szweda⁷, and Hesham A. Sadek^{1,#}

¹Department of Internal Medicine, The University of Texas Southwestern Medical Center, Dallas, Texas 75390, USA

²Department of Molecular Biology, The University of Texas Southwestern Medical Center, Dallas, Texas 75390, USA

³Department of Pediatrics, The University of Texas Southwestern Medical Center, Dallas, Texas 75390, USA

⁶Cardiovascular Division, King's College London BHF Centre of Research Excellence, School of Medicine, James Black Centre, London, SE5 9NU, United Kingdom

⁵Department of Cell Biology, The University of Texas Southwestern Medical Center, Dallas, Texas 75390, USA

⁶Department of Clinical Science, The University of Texas Southwestern Medical Center, Dallas, Texas 75390, USA

⁷Free Radical Biology and Aging Research Program, Oklahoma Medical Research Foundation, Oklahoma City, Oklahoma 73104, USA

⁸Molecular Medicine Laboratory, International Centre for Genetic Engineering and Biotechnology, 34149 Trieste, Italy

⁹Departments of Pathology, University of Washington, Seattle, WA 98195, USA

¹⁰Department of Radiation Oncology, The University of Texas Southwestern Medical Center, Dallas, Texas 75390, USA

© 2014 Elsevier Inc. All rights reserved.

#Corresponding author: hesham.sadek@utsouthwestern.edu.

*These authors contributed equally to this work.

Publisher's Disclaimer: This is a PDF file of an unedited manuscript that has been accepted for publication. As a service to our customers we are providing this early version of the manuscript. The manuscript will undergo copyediting, typesetting, and review of the resulting proof before it is published in its final citable form. Please note that during the production process errors may be discovered which could affect the content, and all legal disclaimers that apply to the journal pertain.

¹¹Cardiovascular Division; Department of Medicine; Brigham and Women's Hospital and Harvard Medical School; Cambridge, MA 02115, USA

Summary

The mammalian heart has a remarkable regenerative capacity for a short period of time after birth, after which the majority of cardiomyocytes permanently exit cell cycle. We sought to determine the primary post-natal event that results in cardiomyocyte cell-cycle arrest. We hypothesized that transition to the oxygen rich postnatal environment is the upstream signal that results in cell cycle arrest of cardiomyocytes. Here we show that reactive oxygen species (ROS), oxidative DNA damage, and DNA damage response (DDR) markers significantly increase in the heart during the first postnatal week. Intriguingly, postnatal hypoxemia, ROS scavenging, or inhibition of DDR all prolong the postnatal proliferative window of cardiomyocytes, while hyperoxemia and ROS generators shorten it. These findings uncover a previously unrecognized protective mechanism that mediates cardiomyocyte cell cycle arrest in exchange for utilization of oxygen dependent aerobic metabolism. Reduction of mitochondrial-dependent oxidative stress should be important component of cardiomyocyte proliferation-based therapeutic approaches.

Introduction

The pathophysiological basis of heart failure is the inability of the adult heart to regenerate lost or damaged myocardium, and although limited myocyte turnover does occur in the adult heart, it is insufficient for restoration of contractile dysfunction (Bergmann et al., 2009; Hsieh et al., 2007; Laflamme et al., 2002; Nadal-Ginard, 2001; Quaini et al., 2002). In contrast, the neonatal mammalian heart is capable of substantial regeneration following injury through cardiomyocyte proliferation (Porrello et al., 2013; Porrello et al., 2011b), not unlike urodele amphibians (Becker et al., 1974; Flink, 2002; Oberpriller and Oberpriller, 1974) or teleost fish (Gonzalez-Rosa et al., 2011; Poss et al., 2002; Wang et al., 2011). However, this regenerative capacity is lost by postnatal day 7 (Porrello et al., 2013; Porrello et al., 2011b), which coincides with cardiomyocyte binucleation and cell cycle arrest (Soonpaa et al., 1996). Although several regulators of cardiomyocytes cell cycle postnatally have been identified (Bersell et al., 2009; Chen et al., 2013; Eulalio et al., 2012; Mahmoud et al., 2013; Porrello et al., 2011a; Sdek et al., 2011; Xin et al., 2013), the upstream signal that causes permanent cell cycle arrest of most cardiomyocytes remains unknown.

One of many factors shared by organisms that are capable of heart regeneration is the oxygenation state. For example, the zebrafish's stagnant and warm aquatic environment has 1/30th oxygen capacitance compared to air, and is prone to poor oxygenation, which may explain the remarkable tolerance of zebrafish to hypoxia (Rees et al., 2001; Roesner et al., 2006). Typical air-saturated water has a PaO₂ of 146mm Hg and zebrafish can tolerate hypoxia at PaO₂ of 15 mmHg (10% air-saturation) for 48 hours, and even 8 mmHg with hypoxic preconditioning. Moreover, the zebrafish circulatory system is relatively hypoxemic, as it has a primitive two-chambers heart with one atrium and one ventricle, which results in mixing of arterial and venous blood.

The mammalian heart has four chambers with no mixing of arterial and venous blood, however during intrauterine life, the mammalian fetal circulation is shunt-dependent with significant arterio-venous mixing of arterial and venous blood. Mixing and shunting of blood occurs at three sites: the ductus venosus, foramen ovale and ductus arteriosus. Blood in the umbilical vein going to the fetus is 80%-90% saturated with a PaO₂ of 32–35mm Hg whereas the fetal venous blood return is quite desaturated at 25–40%. Despite preferential streaming of blood through the shunts to preserve the most oxygenated blood for the brain and the myocardium, the saturation of the blood ejected from the left ventricle is only 65% saturated with a PaO₂ of 25–28mm Hg (Dawes et al., 1954). Therefore, both the zebrafish heart, and the mammalian fetal heart reside in relatively hypoxic environments (Fig. 1A).

Transition from embryonic- to postnatal-circulation soon after birth drastically changes the oxygenation state of cardiomyocytes. For example, arterial pO₂ increases from 30 mm Hg (Lawrence et al., 2008; Mitchell and Van Kainen, 1992; Reynolds et al., 1996) to 100 mm Hg (Webster and Abela, 2007) (Fig. 1A). In parallel, energy metabolism of the embryonic and adult heart is quite distinct. During embryonic development, when cardiomyocytes rapidly proliferate, the relatively hypoxic embryonic heart utilizes anaerobic glycolysis as a main source of energy (Fisher et al., 1980; Lopaschuk et al., 1992), whereas adult cardiomyocytes utilize the oxygen-dependent mitochondrial oxidative phosphorylation as an energy source (Gertz et al., 1988; Wisneski et al., 1985). Nevertheless, the timeframe of this metabolic shift and its relation to cardiomyocyte cell cycle is unknown.

Mitochondrial oxidative phosphorylation produces 18 times as much ATP as cytoplasmic glycolysis (Dismukes et al., 2001; Semenza, 2007). However, the energy advantage of mitochondrial oxidative phosphorylation over glycolysis is not without deleterious consequences, as the mitochondrion is considered the major source of free radical production (Miquel et al., 1980; Turrens, 1997, 2003). Mitochondrial ROS are generated as a consequence of electron leak by the electron transport chain (Koopman et al., 2010; Rudolph and Heyman, 1974) and can cause cellular toxicity by promoting damage of proteins, nucleic acids, lipids or DNA, such as oxidized base, single- or double-strand breaks, resulting in cell cycle arrest, apoptosis or cellular senescence (Hoeijmakers, 2009; Marnett et al., 2003; Moos et al., 2000). The role of mitochondrial ROS, or DNA damage response in postnatal cell cycle arrest of cardiomyocytes is unknown.

Here we show that early postnatal mouse and zebrafish hearts share a low mitochondrial content and complexity, and lack markers of DNA damage response, all of which significantly increase in the postnatal mouse heart within days after birth. Moreover, we show that there is a temporal shift from glycolytic to oxidative metabolism, with a subsequent increase in mitochondrial ROS production, which induces cardiomyocyte cell cycle arrest through activation of the DNA damage response. Systemic scavenging of ROS, specific scavenging of mitochondrial ROS in cardiomyocytes, or inhibition of the DNA damage response pathway, all delay postnatal cell cycle arrest of cardiomyocytes. These findings identify ROS-induced activation of the DNA damage response pathway as an important mediator of cell cycle arrest in postnatal cardiomyocytes.

Results

Mitochondrial characteristics in neonatal and zebrafish hearts

In order to examine relationship between mitochondrial respiration and regenerative potential in vertebrate hearts amongst species, we first examined mitochondrial DNA content in the ventricular chamber of the heart with quantitative RT-PCR (qPCR) over 2 weeks after birth in mouse (n=3) and adult zebrafish (n=3). Mitochondrial DNA copy number compared with nuclear DNA copy number over the weight of ventricle showed a linear increase in the two weeks after birth (Fig. 1B, blue bars). Intriguingly, mitochondrial DNA per gram of tissue was low in adult zebrafish and early neonatal mouse hearts (Fig. 1B) compared to in the hearts of later postnatal age mice. Next, we examined mitochondrial cristae density, an index of increased proton pumping capacity of mitochondria, in adult zebrafish heart (n=3) and neonatal mouse hearts (n=3), using transmission electron microscopy (TEM) imaging. Mitochondrial cristae were sparse in zebrafish and P1 mouse in ventricular cardiomyocytes, but became dense and well-organized at P7 and later postnatal timepoints (Fig. 1C). These results suggest that the increase in mitochondrial mass and complexity correlate temporally with cell cycle arrest of cardiomyocytes.

To further assess capacity of oxidative metabolism in the postnatal mouse heart, we performed comprehensive mass spectrometry-based quantification of enzymes involved in both aerobic and anaerobic metabolism. We found that the majority of the enzymes related to glycolysis were downregulated from P1 to P7, and concomitantly, the majority of the enzymes involved in mitochondrial Krebs cycle were upregulated in the same timeframe (Fig. S1A). Importantly, over 80% of fatty acid beta oxidation enzymes, the main source of energy in mature cardiomyocytes (Lopaschuk et al., 1994), were upregulated from P1 to P7 (Fig. S1A). Finally, we measured mitochondrial NADH oxidase activity, a direct measure of NADH flux through mitochondrial electron transport chain enzymes, and found a significant increase in the same timeframe, from P1 to P7 (Fig. S1B). These results demonstrate that a precise correlation exists between the regenerative zebrafish heart and the early neonatal mouse heart, and outline the precise timeframe of the metabolic switch from anaerobic glycolysis to mitochondrial oxidative phosphorylation in mouse heart within one week after birth.

Activation of DNA damage response pathway in postnatal mouse heart

An important byproduct of mitochondrial respiration is the generation of reactive oxygen species (ROS), which cause cellular oxidative stress, in turn inducing various types of cellular toxicity including widespread damage to proteins, lipids, and nucleic acids (Judge and Leeuwenburgh, 2007). We therefore assess the production of ROS and oxidative stress in postnatal cardiomyocytes. Increase in ROS in cardiomyocytes was directly measured by the detection of dihydroethidium (DHE) oxidation product 2-hydroxyethidine (EOH), which is a marker of superoxide generation, and ethidium (E), which is a marker of hydrogen peroxide (H₂O₂) and other ROS, with high-performance liquid chromatography (HPLC, Fig. 1D (Zhao et al., 2005)). In addition, the fluorescence of ROS indicator dihydrorhodamine 123 (Fig. 1E), as well as 2',7'-dichlorofluorescein {H2DCF (Mills et al., 1998; Sundaresan et al., 1995), Fig. S1C} in fresh non-fixed hearts, further supported the increased ROS levels

in cardiomyocytes after birth. We then examined the glutathione levels in postnatal cardiomyocytes. We found that reduced glutathione (L- γ -glutamyl-L-cysteinylglycine, GSH) and oxidized glutathione disulfide (GSSG) both decreased progressively from P1 to P4 and further at P7 (Fig. S1D). However, GSSG decreased to a greater extent, which resulted in an overall increase in the GSH:GSSH ratio (Fig. S1D). Although the ratio of reduced to oxidized glutathione is widely used as an index of oxidative stress (Schafer and Buettner, 2001), recently the absolute levels of GSSG have been shown to exert significant toxic effects. More importantly, the toxic effects of GSSG are enhanced up to 20 fold in low GSH conditions (Park et al., 2009). As a result, GSSG is readily pumped to the extracellular compartment as a protective mechanism against its toxic effect using an ATP dependent mechanism (Sen et al., 1993). In fact, the decline in the intracellular levels of GSSG is considered a protective mechanism under conditions of oxidative damage. Therefore in the current study, the age depending reduction in GSH, and the further reduction in GSSG are strong indicators of the oxidant environment in the postnatal heart, however it does not seem that there is an overall increased susceptibility to oxidative stress given the elevated GSH:GSSG ratio. In an effort to characterize the endogenous antioxidant response postnatally, we examined the levels of various antioxidant enzymes by quantitative mass spec. We found that mitochondrial superoxide dismutase {SOD2, (Halliwell B, 2007)}, was the only antioxidant enzyme that was significantly increased at P4 and P7 compared to P1, while other antioxidant enzymes failed to increase within the same timeframe (Fig. S1E).

These results led us to hypothesize that oxidative DNA damage caused by ROS may increase in cardiomyocytes postnatally and plays a role in postnatal cell cycle arrest. In order to examine DNA damage in post-natal cardiomyocytes, we assessed and quantified oxidative base modification of DNA by immunostaining using an anti-8-oxo-7,8-dihydroguanine (8-oxoG) antibody. Here we found that nuclear 8-oxoG was undetectable at P1, but significantly increased at P7 and P14 (Fig. 1F, left panels). In concert, the DNA damage response pathway was also significantly activated as indicated by upregulation of phosphorylated-Ataxia Telangiectasia Mutated (pATM), an essential mediator of DNA damage response activation, at P7 and P14 (Fig. 1F, right panels). In addition, further analysis of nuclear 8-oxoG using high resolution confocal microscopy and quantification of oxidized DNA damage foci revealed a significant increase in the number of oxidized DNA damage foci at P4 and P7 compared to P1 (Figure 1G). Also, quantitative analysis of nuclear pATM by western blot showed a significant increase in levels as early as P4, with further increase at P7 compared to P1 (Fig. 1G). Furthermore, quantitative real time PCR analysis for downstream effectors of the DNA damage response pathway also confirmed upregulation of other DNA damage response components including genes involved in damaged DNA binding and repair (Fig. S1F). Interestingly, we found that total ATM mRNA was mildly downregulated, despite the significant upregulation of the active phosphorylated form of ATM. Moreover, and consistent with our previous findings, 8-oxoG was not detectable in zebrafish cardiomyocytes (Fig. S2). These results demonstrate that the increase in mitochondrial respiration corresponds temporally with an increase in ROS in the neonatal heart and activation of DNA damage response.

Environmental oxygen regulates postnatal cardiomyocyte cell cycle arrest

To directly test that whether aerial oxygen can induce postnatal cardiomyocyte cell cycle arrest, we exposed neonates to hyperoxic (100% O₂) or mildly hypoxic (15% O₂) environment starting at E18.5 (n=3 each, Fig. 2A). Remarkably, oxidative DNA damage and the activation of DDR was accelerated in P4 hyperoxia heart, and in contrast, was repressed in P7 hypoxia heart (Fig. 2B). Heart weight to body weight (HW/BW) ratio was normal in neonates under hyperoxia, whereas significantly increased in those under hypoxia (Fig. 2C). Normally, postnatal heart growth is achieved by hypertrophic growth rather than hyperplastic growth after the first week of life (Porrello et al., 2008). Wheat germ agglutinin (WGA) staining and cell size quantification with imageJ revealed significant decrease in cardiomyocyte cell size after hypoxia treatment, although hyperoxic treatment did not change the size (Fig. 2D). The presence of phosphorylated histone H3 Ser 10 (pH3), a marker of G2-M progression, was significantly decreased in cardiomyocyte after hyperoxia treatment, and in contrast increased after hypoxia treatment (Fig. 2E). In addition, localization of Aurora B kinase at the cleavage furrow, a marker for cytokinesis, was decreased in hyperoxic hearts and mildly increased in hypoxic hearts (Fig. 2F). These results strongly indicate that perinatal and postnatal oxygen concentration affects cardiomyocyte proliferation in neonates. We therefore further hypothesized that the exposure to aerial oxygen induces cardiomyocyte cell cycle arrest after birth through oxidative stress and intracellular stress response pathway.

Reactive oxygen species induce postnatal cardiomyocyte cell cycle arrest

To assess the contribution of oxidative stress to cell cycle arrest of post-natal cardiomyocyte, we injected the ROS generator diquat (5mg/kg) daily for 3 days after birth (n=3, Fig. 3A). Strong induction of oxidative DNA damage indicated by 8-oxoG (Fig. 3B) was observed, and although HW/BW ratio was unchanged (Fig. 3C), we found that the size of individual cardiomyocytes was significantly increased (Fig. 3D). In addition, cardiomyocyte mitosis assessed by anti-pH3 staining was drastically reduced in cardiomyocytes in the diquat injected neonates (Fig. 3E). TUNEL assay showed no increase in apoptotic cardiomyocyte cell death after diquat treatment (Fig. 3E). Finally, cardiomyocyte cytokinesis assessed by anti-Aurora B staining was also significantly decreased in the hearts of diquat injected neonates (Fig. 3F). These findings were further confirmed with the injection of another ROS generator paraquat (5mg/kg, n=3, Fig. S3A). The injection of paraquat induced an increase in cardiomyocyte cell size (Fig. S3B), and a decrease in cardiomyocyte mitosis, without significant increase in apoptosis (Fig. S3C). Cardiomyocyte cytokinesis was consistently decreased with paraquat injection (Fig. S3D). Moreover, we directly injected 30µl of 1µM H₂O₂ into the apex of P1 mouse hearts (n=3, Fig. S4A). Two days after H₂O₂ injection, strong induction of phosphorylated ATM was observed (Fig. S4B), and although heart weight to body weight ratio was in normal range (Fig. S4C), the size of individual cardiomyocytes was significantly increased (Fig. S4D). In addition, cardiomyocyte mitosis was almost completely lost in the H₂O₂ treated hearts throughout the entire myocardium (Fig. S4E). Although a significant increase in apoptotic cardiomyocyte cell death was shown in the direct H₂O₂ injected hearts, the vast majority of the TUNEL positive cells were along the needle track, while the effect on myocyte proliferation was global throughout the myocardium (Fig. S4F). In combination, these

results strongly indicate that ROS can induce a shift from hyperplastic to hypertrophic growth in the postnatal mammalian heart. It is important to note here that although there is a clear inhibitory effect on cell cycle in the absence of increased cell death, the physiological relevance if these stimuli is less certain because we are unable to control the amount or cellular localization of ROS production.

Scavenging reactive oxygen species prolongs postnatal cardiomyocyte proliferation

To test whether scavenging ROS can extend cardiomyocyte proliferation after birth, we administered N-acetylcysteine (NAC) daily for two weeks after birth (n=3, Fig. 4A). Staining with dihydrorhodamine 123 showed a decreased cellular ROS level after NAC treatment (Fig. 4B). Detection of the DHE products with HPLC also indicates that both superoxides and other ROS were significantly reduced upon NAC treatment (Fig. S6A). Accordingly, the level of 8-oxoG (Fig. 4C) and phosphorylated ATM (Fig. 4D) were markedly decreased in cardiomyocyte nuclei after a 1 week treatment with NAC, indicating that oxidative DNA damage and the activation of the DDR by oxidative stress was suppressed. Although HW/BW ratio was normal (Fig. 4E), cardiomyocyte cell size was significantly decreased in NAC treated neonates (Fig. 4F). This suggests that NAC treatment delays the postnatal switch from hyperplastic to hypertrophic growth. To confirm this finding, we performed a number of additional studies. First, we observed that NAC treatment increased the total number of cardiomyocytes (Fig. 4G). We next examined cardiomyocyte proliferation in NAC treated hearts. Immunostaining with anti-pH3 antibody revealed a significant increase in cardiomyocyte mitosis in the NAC treated hearts compared to control hearts at both P7 and P14 (Fig. 4H). Moreover, we found that cardiomyocyte cytokinesis was significantly increased as determined by an increase in the number of Aurora B positive cardiomyocytes in the NAC treated hearts (Fig. 4I). In addition, we found that the NAC treated hearts had significantly less binucleated cardiomyocytes compared to control hearts (Fig. 4J). It is important here to note that we used very stringent immunohistochemical methods for these measurements, including the use of WGA staining to delineate the borders of myocytes to avoid counting non-myocyte nuclei, as well as confocal z-stacking to confirm the location of pH3 and Aurora B. Finally, TUNEL assay showed no increase in cell death (Fig. 4K). In addition, NAC treatment on isolated neonatal rat cardiomyocytes significantly increased DNA synthesis and mitosis, and also reduced polyploidy (Fig. S5). However, we noted that cardiomyocyte proliferation gradually decreased over time in the NAC treated heart within one month after birth (data not shown). qPCR and quantitative mass spec analyses showed little change in levels of proteins involved in oxidative phosphorylation in the NAC treated p7 hearts compared to control p7 hearts (Fig. S6A). The measurement of NADH oxidase activity revealed increase in mitochondrial respiration at P7 even upon NAC administration (Fig. S6C). Overall, these results indicate that scavenging ROS extends the time window of postnatal cardiomyocyte proliferation in the postnatal mouse heart and are consistent with a model in which an increase in reactive oxygen species triggers cardiomyocyte cell cycle arrest shortly after birth.

Mitochondrial-specific scavenging of ROS induces postnatal cardiomyocyte proliferation

To selectively examine whether mitochondrial ROS production is involved in postnatal cell cycle arrest of cardiomyocytes, we utilized a genetic model to over-express a radical scavenger specifically in cardiomyocyte mitochondria. We crossed floxed-stop mCAT (mitochondrial-specific catalase) mice, in which floxed transcriptional stop sequences are inserted in between universal GAPDH enhancer/promoter and mitochondrial-targeted catalase {mCAT (Dai et al., 2011; Schriener et al., 2005)}, with Myh6-Cre mice, to generate mice expressing mCAT only in cardiomyocytes by cardiomyocyte specific deletion of floxed stop with Myh6 enhancer/promoter driven Cre recombinase (hereinafter called mCAT mice, Fig. 5A). We confirmed that in mCAT mice the level of ROS was decreased with direct staining with dihydrorhodamine 123 (Fig. 5B) compared with control Myh6-Cre mice. Quantification of ROS in the heart by HPLC detection of EOH peak showed no significant change in the level of superoxide, whereas a significant reduction in the E peak, indicative of substantial decrease in H₂O₂ (as expected given that catalase primarily acts on H₂O₂, Fig. S6B). Accordingly, oxidative DNA damage (Fig. 5C) and the activation of DDR pathway (Fig. S6E) were suppressed. In mCAT mice, HW/BW ratio was normal (Fig. 5D), however, cardiomyocyte cell size in mCAT mice at P14 was significantly smaller than that in control mice (Fig. 5E). In addition, cardiomyocyte mitosis (Fig. 5F), as well as cytokinesis (Fig. 5G), were increased in mCAT hearts. Accordingly, the total number of cardiomyocyte in mCAT mice was significantly increased in comparison with that in control mice (Fig. 5H). The number of proliferative mononucleated cardiomyocytes was increased and binucleated cardiomyocytes were decreased in mCAT heart (Fig. 5I). Cardiomyocyte apoptosis was in the normal range in mCAT heart (Fig. 5J). These results strongly suggest that mitochondrial ROS production induces postnatal cell cycle arrest of cardiomyocytes.

NAC injection improves cardiac function after injury

We next tested whether radical scavenging can extend the regenerative potential of mammalian heart. We injected NAC daily after birth and induced ischemia reperfusion (IR) injury at P21 (n=12), a time-point well beyond the P7 where the postnatal heart loses its regenerative potential (Fig. 6A). It is important to note here that the control mice also received NAC at the time of IR injury to equalize any effect of NAC injection of ROS induced infarct expansion following ischemia reperfusion. Cardiomyocyte viability assessed with 2,3,5-trimethyl tetrazolium chloride (TTC) staining was not significantly different between long-term NAC treated and control hearts (n=3, Fig. 6B). One week and 1 month after the IR injury, there was no significant change in heart size in the NAC treated animals (Fig. 6C). WGA staining showed a significant decrease in cardiomyocyte cell size at 1 month after IR injury, which along with the unchanged HW/BW suggests that the NAC treated hearts have more cardiomyocytes (Fig. 6D). In addition, systolic function assessed by ejection fraction (EF) and fraction shortening (SF) was significantly improved in the NAC treated group (Fig. 6E). Fibrotic scar formation was also decreased after NAC treatment (Fig. 6F). Finally, by assessing the number of pH3 positive cardiomyocyte at 3 days after IR (Fig. 6G) and BrdU incorporation into cardiomyocytes nuclei at 7 days after IR (Fig. 6H), we showed that cardiomyocyte proliferation was significantly increased in the NAC treated hearts. These data indicate that scavenging ROS can extend regenerative potential of the heart beyond 1 week after birth. It is important here to note that there may be

several effects of NAC going on concomitantly; for example although we administered NAC to the control group for a short period of time after injury in an attempt counteract any effect of NAC on ROS mediated reperfusion injury, it is likely that the continued NAC administration over 1 month also resulted in decreased cardiomyocyte loss and remodeling following injury.

Pharmacological inhibition of DNA damage response pathway extends the window of cardiomyocyte proliferation in the postnatal mouse heart

Once cells are subjected to DNA damage, cell cycle checkpoint pathways are activated to arrest cells in G1 or G2 phases (Elledge, 1996; Sherr, 1996). In order to determine whether DNA damage-induced activation of cell cycle checkpoint pathway is involved in cardiomyocytes cell cycle arrest, we examined the Wee1-dependent activation of G2-M cell cycle checkpoint in postnatal cardiomyocytes. Activation of ATM or ATR kinase in response to DNA damage in turn activate Wee1 kinase, a repressor of CDK1 dependent G2-M transition (Fig. 7A, (Heald et al., 1993; Parker and Piwnica-Worms, 1992; Santamaria et al., 2007)). We performed immunostaining with anti-Wee1 antibody and showed that nuclear wee1 protein was absent from cardiomyocyte nuclei immediately after birth, but became strongly expressed at P7 as well as P14 (Fig. 7B, left). The level of Wee1 protein drastically increased in the heart at p4 compared to that at P1, and rose further at P7 (Fig. 7B, right). To test whether Wee1 plays a role in postnatal cardiomyocyte cell cycle arrest, we inhibited Wee1 kinase activity pharmacologically. We injected Wee1 inhibitor MK-1775, for which several clinical trials is now ongoing as a cancer treatment drug and several of them are now in phase II (NCT01164995, NCT01357161, NCT01827384), daily from birth till 2 weeks of age (n=3, Fig. 7C). Wee1 inhibition resulted in a trend towards decrease in heart size, which was not statistically significant (Fig. 7D). Notably, Wee1 inhibitor treated hearts showed robust induction of cardiomyocyte proliferation at p14 indicated by both anti-pH3 (Fig. 7E) and anti-Aurora B (Fig. 7G) immunostaining, as well as reduced cardiomyocyte cell size (Fig. 7F). TUNEL assay showed no increase in apoptotic cell death in Wee1 inhibitor treated hearts (Fig. 7H). Moreover, total number of cardiomyocytes in Wee1 inhibitor treated P14 hearts was significantly increased both at P7 and at P14 (Fig. 7I), and cardiomyocyte binucleation was inhibited in the Wee1 inhibitor treated hearts (Fig. 7J). Furthermore, Wee1 was downregulated when ROS was scavenged in NAC injected or mCAT mice (Fig. S6B) at P7. These data strongly suggest that Wee1 mediates postnatal cardiomyocyte cell cycle arrest in mouse heart, and that blocking Wee1 kinase dependent signaling is sufficient to extend the timing of the postnatal switch from hyperplastic to hypertrophic myocyte growth in the heart.

In summary, our results indicate that a postnatal increase in mitochondrial-derived reactive oxygen species induces cell cycle arrest through activation of the DNA damage response pathway in mouse heart within 7 days after birth. Moreover, it is intriguing that the oxidation status and regenerative capacity are well correlated amongst regenerative lower vertebrates and the early postnatal mammalian heart.

Discussion

One of the long-standing mysteries in cardiovascular biology is the permanent cell cycle arrest of adult cardiomyocytes, both from an etiological as well as mechanistic perspective. From a mechanistic perspective, several regulators of cardiomyocyte cell cycle have been identified (Agah et al., 1997; Bersell et al., 2009; Chen et al., 2013; Eulalio et al., 2012; Jackson et al., 1990; Liao et al., 2001; Liu et al., 2010; Mahmoud et al., 2013; Porrello et al., 2011a; Reiss et al., 1996; Sdek et al., 2011; Xin et al., 2013), including both direct and indirect cell cycle regulators. However, the upstream event that triggers these cascades is unknown. A more important question is why are adult cardiomyocytes unable to re-enter cell cycle on demand, for example after injury? In the current report, we show that the increase in environmental oxygen, and the subsequent upregulation of oxidative metabolism is the upstream signal that triggers cell cycle exit of cardiomyocytes shortly after birth.

In the immediate postnatal period, mammalian hearts predominantly rely on glycolysis and lactate fermentation as sources of ATP, (Lopaschuk and Jaswal, 2010; Lopaschuk et al., 1991; Werner and Sicard, 1987) whereas there is only minor contributions of fatty acid beta-oxidation to total myocardial ATP production (Lopaschuk et al., 1991). This reliance on glycolysis is very similar to that found in fetal heart (Lopaschuk et al., 1992; Makinde et al., 1998). However, within a very short period of time after birth, anaerobic glycolysis is decreases markedly (Lopaschuk and Spafford, 1990; Lopaschuk et al., 1991) with a significant increase in mitochondrial metabolism and fatty acid beta-oxidation (Ascuitto et al., 1989; Lopaschuk and Spafford, 1990; Werner and Sicard, 1987). While pioneering reports correctly identified the metabolic shift that occurs after birth, our current work outlines the precise timeframe of postnatal upregulation in mitochondrial mass as well as the change in protein levels of the majority of components of these pathways. These changes directly correlate with the postnatal exit of cardiomyocytes from the cell cycle.

Moreover, we provide multiple levels of evidence to support our hypothesis that increased environmental oxygen; with the subsequent increase in mitochondrial oxidative metabolism, induce cardiomyocyte cell cycle arrest through activation of the DNA damage response. First, we show that the regenerative zebrafish heart, similar to the early postnatal mouse heart have very low mitochondrial content and complexity, and show no evidence of activation of the DDR pathway. Second, we show that the postnatal increase in mitochondrial mass, complexity, and activity, increased ROS, increased markers of DNA damage, and activation of DDR pathway, all correlate temporally with cell cycle exit of cardiomyocytes. Third, we show that postnatal hypoxemia inhibits DNA damage and prolongs the postnatal window of cardiomyocytes proliferation, while postnatal hyperoxemia potentiates DNA damage and early cell cycle arrest. Fourth, we show that ROS generators induce DDR and early cell cycle arrest, while both non-specific and mitochondrial-targeted ROS scavenging delays activation of the DNA damage response and delays cell cycle arrest of cardiomyocytes. Finally, we show that pharmacological inhibition of the DDR pathway prolongs the postnatal window of cardiomyocyte proliferation. It is important to note here that although we were able to prolong the postnatal window of myocyte proliferation with ROS scavenging, we were unable to prevent cell cycle arrest. The inevitable cell cycle exit of cardiomyocyte is likely multifactorial and possibly related

to our inability to completely prevent DNA damage, or other factors such as the postnatal change in type and abundance of nutrients (Siggins et al., 2012), or increased hemodynamic stress. Similarly, pharmacological inhibition of wee1 delayed, but did not prevent, cell cycle arrest. This is perhaps not surprising given the downstream cell cycle targets of the DDR pathway that do not involve wee1, which regulates cyclin B/CDK1, while cyclin E/CDK2 is targeted by other components of the DDR pathways.

The effect of ROS on cell cycle is complex, and probably greatly influenced by level, source, type, compartmentalization and duration of exposure to ROS. Evidence suggests that ROS can be pro-proliferative in several scenarios (Jang and Sharkis, 2007; Leslie, 2006; Myant et al., 2013; Tothova et al., 2007), and can stimulate differentiation of several cell types (Lee et al., 2005; Owusu-Ansah and Banerjee, 2009; Tsatmali et al., 2006) including cardiomyocytes. *In vitro* studies using embryonic stem (ES) cells have shown that redox balance is a critical regulator of cardiomyocyte differentiation (Birket et al., 2013; Buggisch et al., 2007; Sauer et al., 2000). ROS mediates mechanical strain and electrical stimulation-induced cardiomyocyte differentiation of ES cells (Puceat et al., 2003; Schmelter et al., 2006), while ROS scavengers impair cardiomyocyte formation in embryoid bodies (Li et al., 1996; Pi et al., 2013; Sauer et al., 2000; Yoneyama et al., 2010). In contrast, ROS mediated senescence and cell cycle exit is a well-recognized characteristic of stem cells (Takahashi et al., 2006; Trachootham et al., 2009).

The current report demonstrates that the neonatal mouse heart and the zebrafish heart may have more in common than previously recognized. The hypoxic nature of the zebrafish external and circulatory environments prevent activation of the DDR and cell cycle arrest of myocytes. In support of this notion, additional hypoxia actually enhances myocyte proliferation and regenerative capacity of zebrafish hearts (Jopling et al., 2012; Marques et al., 2008), and in the current report, prolongs the postnatal window of myocyte proliferation in mammals. Shortly after birth, the metabolic switch that occurs in the mammalian heart confers significant energy efficiency through oxidative metabolism, unfortunately at the expense of proliferative competency. We conclude that mitochondrial ROS mediated activation of the DDR is an important upstream event that mediates cell cycle arrest of postnatal cardiomyocytes.

Experimental Procedures

Animal breeding and genotyping

All protocols were approved by the Institutional Animal Care and Use Committee of the University of Texas Southwestern Medical Center. All experiments were performed on age and sex matched mice, with equal ratio of male to female mice. The number of animals used for each experiment; n=3. Transgenic mCAT mice were kindly provided by Dr. Ravinovitch. Mice were genotyped as described previously (Dai et al., 2011; Schriener et al., 2005).

Drug injection

N-Acetyl-L-cysteine (Sigma) were reconstituted in PBS to concentrations of 10mg/ml. CD-1 (Charles River) mice were weighed daily and 75mg/kg were injected daily subcutaneously or intra-peritoneal from day 0 to day 14. Wee1-inhibitors (MK-1775, Selleck) were reconstituted in diluted DMSO. CD-1 mice were injected daily with 2.5mg/kg subcutaneously or intra-peritoneal from day 0 to day 14. Diquat, paraquat and H₂O₂ were diluted in PBS and injected into CD-1 neonates as described in Results.

Histology

Hearts were harvested and fixed in 4% paraformaldehyde (PFA)/PBS solution overnight at room temperature and then processed for paraffin sectioning. Masson's trichrome staining was performed according to standard procedures at UTSW core histology facility on paraffin sections. TUNEL staining was performed according to manufacturer's recommendations (*In-Situ* Cell Death Detection Kit, Fluorescein, Cat# 11684795910, Roche).

Immunostaining

Following antigen retrieval with 1mM EDTA in boiling water, sections were blocked with 10% serum from host animal of secondary antibodies, and incubated with primary antibodies overnight at 4°C. Sections were subsequently washed with PBS and incubated with corresponding secondary antibodies conjugated to Alexa Fluor 350, 488 or 555 (Invitrogen). Primary antibodies used are following: anti-phospho Histone H3 Ser10 (Millipore #06-570, 1:100), anti-Aurora B (Sigma A5102, 1:100), anti-Troponin T, Cardiac Isoform Ab-1, Clone 13-11 (Thermo scientific MS-295-P1, 1:100), anti-Bromodeoxyuridine (Roche #11170376001, 1:25), anti-Sarcomeric Alpha Actinin (Abcam, ab68167, 1:100), anti-oxoguanine 8 (Abcam Ab64548, 1:100), anti-phosphorylated ATM (Santa Cruz Biotechnology sc-47739, 1:100), anti-Wee1 (Abcam ab137377, 1:100). Anti-weat germ agglutinin (WGA) conjugated to Alexa Fluor 488 (50 µg/ml, Invitrogen).

Cardiomyocyte Isolation

The isolation of cardiomyocyte from neonatal hearts and staining with anti-connexin 43 antibody were performed as previously described (Mahmoud et al., 2013).

Reactive oxygen species determination

Dihydrorhodamine 123 (Life Technologies, D-23806) or CM-H2DCFDA (Life Technologies, C6827) and HPLC detection of DHE were used to detect ROS. See Extended Experimental Procedures for detailed methods.

Cristae measurement

Spacings between cristae in individual mitochondria were quantified using ImageJ. Only mitochondria with several well defined, parallel cristae were selected for analysis. The ImageJ line tool was used to draw a line across the stack of cristae, perpendicular to the orientation of the cristae, and the number of cristae crossing the line was counted

interactively. The pixel size defined in the image metadata was used to obtain the length of the line profile in μm .

Western blotting

Western blot was performed using standard protocols. See Extended Experimental Procedures for detailed methods.

Statistical Analysis

1-tailed or 2-tailed Student's *t* test was used to determine statistical significance and $*p < 0.05$ and $**p < 0.01$ was considered statistically different. All quantification is blinded.

Supplementary Material

Refer to Web version on PubMed Central for supplementary material.

Acknowledgments

We thank Dr. James Richardson and John Shelton for their valuable input. This work is supported by NASA grant # NNX13AD57G (Aroumougame), Advanced Grant 20090506 from the European Research Council (ERC) (Giacca), British Heart Foundation and a Fondation Leducq Transatlantic Network (Shah), as well as grants from the American Heart Association (Grant in Aid), Foundation for Heart Failure Research, NY and the NIH (1R01HL115275-01) (Sadek).

References

- Agah R, Kirshenbaum LA, Abdellatif M, Truong LD, Chakraborty S, Michael LH, Schneider MD. Adenoviral delivery of E2F-1 directs cell cycle reentry and p53-independent apoptosis in postmitotic adult myocardium in vivo. *J Clin Invest*. 1997; 100:2722–2728. [PubMed: 9389735]
- Ascutto RJ, Ross-Ascutto NT, Chen V, Downing SE. Ventricular function and fatty acid metabolism in neonatal piglet heart. *Am J Physiol*. 1989; 256:H9–H15. [PubMed: 2912201]
- Becker RO, Chapin S, Sherry R. Regeneration of the ventricular myocardium in amphibians. *Nature*. 1974; 248:145–147. [PubMed: 4818918]
- Bergmann O, Bhardwaj RD, Bernard S, Zdunek S, Barnabe-Heider F, Walsh S, Zupicich J, Alkass K, Buchholz BA, Druid H, et al. Evidence for cardiomyocyte renewal in humans. *Science*. 2009; 324:98–102. [PubMed: 19342590]
- Bersell K, Arab S, Haring B, Kuhn B. Neuregulin1/ErbB4 signaling induces cardiomyocyte proliferation and repair of heart injury. *Cell*. 2009; 138:257–270. [PubMed: 19632177]
- Birket MJ, Casini S, Kosmidis G, Elliott DA, Gerencser AA, Baartscheer A, Schumacher C, Mastroberardino PG, Elefanty AG, Stanley EG, et al. PGC-1 α and Reactive Oxygen Species Regulate Human Embryonic Stem Cell-Derived Cardiomyocyte Function. *Stem Cell Reports*. 2013; 1:560–574. [PubMed: 24371810]
- Buggisch M, Ateghang B, Ruhe C, Strobel C, Lange S, Wartenberg M, Sauer H. Stimulation of ES-cell-derived cardiomyogenesis and neonatal cardiac cell proliferation by reactive oxygen species and NADPH oxidase. *J Cell Sci*. 2007; 120:885–894. [PubMed: 17298980]
- Chen J, Huang ZP, Seok HY, Ding J, Kataoka M, Zhang Z, Hu X, Wang G, Lin Z, Wang S, et al. mir-17-92 cluster is required for and sufficient to induce cardiomyocyte proliferation in postnatal and adult hearts. *Circ Res*. 2013; 112:1557–1566. [PubMed: 23575307]
- Dai DF, Johnson SC, Villarín JJ, Chin MT, Nieves-Cintrón M, Chen T, Marcinek DJ, Dorn GW, Kang YJ 2nd, Prolla TA, et al. Mitochondrial oxidative stress mediates angiotensin II-induced cardiac hypertrophy and Galphaq overexpression-induced heart failure. *Circ Res*. 2011; 108:837–846. [PubMed: 21311045]

- Dawes GS, Mott JC, Widdicombe JG. The foetal circulation in the lamb. *J Physiol*. 1954; 126:563–587. [PubMed: 13222355]
- Dismukes GC, Klimov VV, Baranov SV, Kozlov YN, DasGupta J, Tyryshkin A. The origin of atmospheric oxygen on Earth: the innovation of oxygenic photosynthesis. *Proc Natl Acad Sci U S A*. 2001; 98:2170–2175. [PubMed: 11226211]
- Elledge SJ. Cell cycle checkpoints: preventing an identity crisis. *Science*. 1996; 274:1664–1672. [PubMed: 8939848]
- Eulalio A, Mano M, Dal Ferro M, Zentilin L, Sinagra G, Zacchigna S, Giacca M. Functional screening identifies miRNAs inducing cardiac regeneration. *Nature*. 2012; 492:376–381. [PubMed: 23222520]
- Fisher DJ, Heymann MA, Rudolph AM. Myocardial oxygen and carbohydrate consumption in fetal lambs in utero and in adult sheep. *Am J Physiol*. 1980; 238:H399–H405. [PubMed: 7369385]
- Flink IL. Cell cycle reentry of ventricular and atrial cardiomyocytes and cells within the epicardium following amputation of the ventricular apex in the axolotl, *Amblystoma mexicanum*: confocal microscopic immunofluorescent image analysis of bromodeoxyuridine-labeled nuclei. *Anat Embryol (Berl)*. 2002; 205:235–244. [PubMed: 12107494]
- Gertz EW, Wisneski JA, Stanley WC, Neese RA. Myocardial substrate utilization during exercise in humans. Dual carbon-labeled carbohydrate isotope experiments. *J Clin Invest*. 1988; 82:2017–2025. [PubMed: 3198763]
- Gonzalez-Rosa JM, Martin V, Peralta M, Torres M, Mercader N. Extensive scar formation and regression during heart regeneration after cryoinjury in zebrafish. *Development*. 2011; 138:1663–1674. [PubMed: 21429987]
- Halliwell, BGJ. *Free Radicals in Biology and Medicine*. Oxford University Press; 2007.
- Heald R, McLoughlin M, McKeon F. Human wee1 maintains mitotic timing by protecting the nucleus from cytoplasmically activated Cdc2 kinase. *Cell*. 1993; 74:463–474. [PubMed: 8348613]
- Hoeijmakers JH. DNA damage, aging, and cancer. *N Engl J Med*. 2009; 361:1475–1485. [PubMed: 19812404]
- Hsieh PC, Segers VF, Davis ME, MacGillivray C, Gannon J, Molkenkin JD, Robbins J, Lee RT. Evidence from a genetic fate-mapping study that stem cells refresh adult mammalian cardiomyocytes after injury. *Nat Med*. 2007; 13:970–974. [PubMed: 17660827]
- Jackson T, Allard MF, Sreenan CM, Doss LK, Bishop SP, Swain JL. The c-myc proto-oncogene regulates cardiac development in transgenic mice. *Mol Cell Biol*. 1990; 10:3709–3716. [PubMed: 1694017]
- Jang YY, Sharkis SJ. A low level of reactive oxygen species selects for primitive hematopoietic stem cells that may reside in the low-oxygenic niche. *Blood*. 2007; 110:3056–3063. [PubMed: 17595331]
- Jopling C, Sune G, Faucherre A, Fabregat C, Izpisua Belmonte JC. Hypoxia induces myocardial regeneration in zebrafish. *Circulation*. 2012; 126:3017–3027. [PubMed: 23151342]
- Judge S, Leeuwenburgh C. Cardiac mitochondrial bioenergetics, oxidative stress, and aging. *Am J Physiol Cell Physiol*. 2007; 292:C1983–H1992. [PubMed: 17344313]
- Koopman WJ, Nijtmans LG, Dieteren CE, Roestenberg P, Valsecchi F, Smeitink JA, Willems PH. Mammalian mitochondrial complex I: biogenesis, regulation, and reactive oxygen species generation. *Antioxid Redox Signal*. 2010; 12:1431–1470. [PubMed: 19803744]
- Laflamme MA, Myerson D, Saffitz JE, Murry CE. Evidence for cardiomyocyte repopulation by extracardiac progenitors in transplanted human hearts. *Circ Res*. 2002; 90:634–640. [PubMed: 11934829]
- Lawrence J, Xiao D, Xue Q, Rejali M, Yang S, Zhang L. Prenatal nicotine exposure increases heart susceptibility to ischemia/reperfusion injury in adult offspring. *J Pharmacol Exp Ther*. 2008; 324:331–341. [PubMed: 17947495]
- Lee NK, Choi YG, Baik JY, Han SY, Jeong DW, Bae YS, Kim N, Lee SY. A crucial role for reactive oxygen species in RANKL-induced osteoclast differentiation. *Blood*. 2005; 106:852–859. [PubMed: 15817678]
- Leslie NR. The redox regulation of PI 3-kinase-dependent signaling. *Antioxid Redox Signal*. 2006; 8:1765–1774. [PubMed: 16987030]

- Li F, Wang X, Capasso JM, Gerdes AM. Rapid transition of cardiac myocytes from hyperplasia to hypertrophy during postnatal development. *J Mol Cell Cardiol.* 1996; 28:1737–1746. [PubMed: 8877783]
- Liao HS, Kang PM, Nagashima H, Yamasaki N, Usheva A, Ding B, Lorell BH, Izumo S. Cardiac-specific overexpression of cyclin-dependent kinase 2 increases smaller mononuclear cardiomyocytes. *Circ Res.* 2001; 88:443–450. [PubMed: 11230113]
- Liu Z, Yue S, Chen X, Kubin T, Braun T. Regulation of cardiomyocyte polyploidy and multinucleation by CyclinG1. *Circ Res.* 2010; 106:1498–1506. [PubMed: 20360255]
- Lopaschuk GD, Belke DD, Gamble J, Itoi T, Schonekess BO. Regulation of fatty acid oxidation in the mammalian heart in health and disease. *Biochim Biophys Acta.* 1994; 1213:263–276. [PubMed: 8049240]
- Lopaschuk GD, Collins-Nakai RL, Itoi T. Developmental changes in energy substrate use by the heart. *Cardiovasc Res.* 1992; 26:1172–1180. [PubMed: 1288863]
- Lopaschuk GD, Jaswal JS. Energy metabolic phenotype of the cardiomyocyte during development, differentiation, and postnatal maturation. *J Cardiovasc Pharmacol.* 2010; 56:130–140. [PubMed: 20505524]
- Lopaschuk GD, Spafford MA. Energy substrate utilization by isolated working hearts from newborn rabbits. *Am J Physiol.* 1990; 258:H1274–H1280. [PubMed: 2337162]
- Lopaschuk GD, Spafford MA, Marsh DR. Glycolysis is predominant source of myocardial ATP production immediately after birth. *Am J Physiol.* 1991; 261:H1698–H1705. [PubMed: 1750528]
- Mahmoud AI, Kocabas F, Muralidhar SA, Kimura W, Koura AS, Thet S, Porrello ER, Sadek HA. Meis1 regulates postnatal cardiomyocyte cell cycle arrest. *Nature.* 2013; 497:249–253. [PubMed: 23594737]
- Makinde AO, Kantor PF, Lopaschuk GD. Maturation of fatty acid and carbohydrate metabolism in the newborn heart. *Mol Cell Biochem.* 1998; 188:49–56. [PubMed: 9823010]
- Marnett LJ, Riggins JN, West JD. Endogenous generation of reactive oxidants and electrophiles and their reactions with DNA and protein. *J Clin Invest.* 2003; 111:583–593. [PubMed: 12618510]
- Marques IJ, Leito JT, Spaink HP, Testerink J, Jaspers RT, Witte F, van den Berg S, Bagowski CP. Transcriptome analysis of the response to chronic constant hypoxia in zebrafish hearts. *J Comp Physiol B.* 2008; 178:77–92. [PubMed: 17828398]
- Mills EM, Takeda K, Yu ZX, Ferrans V, Katagiri Y, Jiang H, Lavigne MC, Leto TL, Guroff G. Nerve growth factor treatment prevents the increase in superoxide produced by epidermal growth factor in PC12 cells. *J Biol Chem.* 1998; 273:22165–22168. [PubMed: 9712826]
- Miquel J, Economos AC, Fleming J, Johnson JE Jr. Mitochondrial role in cell aging. *Exp Gerontol.* 1980; 15:575–591. [PubMed: 7009178]
- Mitchell JA, Van Kainen BR. Effects of alcohol on intrauterine oxygen tension in the rat. *Alcohol Clin Exp Res.* 1992; 16:308–310. [PubMed: 1590552]
- Moos PJ, Edes K, Fitzpatrick FA. Inactivation of wild-type p53 tumor suppressor by electrophilic prostaglandins. *Proc Natl Acad Sci U S A.* 2000; 97:9215–9220. [PubMed: 10908664]
- Myant KB, Cammareri P, McGhee EJ, Ridgway RA, Huels DJ, Cordero JB, Schwitalla S, Kalna G, Ogg EL, Athineos D, et al. ROS production and NF-kappaB activation triggered by RAC1 facilitate WNT-driven intestinal stem cell proliferation and colorectal cancer initiation. *Cell Stem Cell.* 2013; 12:761–773. [PubMed: 23665120]
- Nadal-Ginard B. [Generation of new cardiomyocytes in the adult heart: Prospects of myocardial regeneration as an alternative to cardiac transplantation]. *Rev Esp Cardiol.* 2001; 54:543–550. [PubMed: 11412743]
- Oberpriller JO, Oberpriller JC. Response of the adult newt ventricle to injury. *J Exp Zool.* 1974; 187:249–253. [PubMed: 4813417]
- Owusu-Ansah E, Banerjee U. Reactive oxygen species prime *Drosophila* haematopoietic progenitors for differentiation. *Nature.* 2009; 461:537–541. [PubMed: 19727075]
- Park HA, Khanna S, Rink C, Gnyawali S, Roy S, Sen CK. Glutathione disulfide induces neural cell death via a 12-lipoxygenase pathway. *Cell Death Differ.* 2009; 16:1167–1179. [PubMed: 19373248]

- Parker LL, Piwnicka-Worms H. Inactivation of the p34cdc2-cyclin B complex by the human WEE1 tyrosine kinase. *Science*. 1992; 257:1955–1957. [PubMed: 1384126]
- Pi Y, Zhang LL, Li BH, Guo L, Cao XJ, Gao CY, Li JC. Inhibition of reactive oxygen species generation attenuates TLR4-mediated proinflammatory and proliferative phenotype of vascular smooth muscle cells. *Lab Invest*. 2013; 93:880–887. [PubMed: 23774581]
- Porrello ER, Johnson BA, Aurora AB, Simpson E, Nam YJ, Matkovich SJ, Dorn GW 2nd, van Rooij E, Olson EN. MiR-15 family regulates postnatal mitotic arrest of cardiomyocytes. *Circ Res*. 2011a; 109:670–679. [PubMed: 21778430]
- Porrello ER, Johnson BA, Aurora AB, Simpson E, Nam YJ, Matkovich SJ, Dorn GW 2nd, van Rooij E, Olson EN. MiR-15 family regulates postnatal mitotic arrest of cardiomyocytes. *Circ Res*. 2013; 109:670–679. [PubMed: 21778430]
- Porrello ER, Mahmoud AI, Simpson E, Hill JA, Richardson JA, Olson EN, Sadek HA. Transient regenerative potential of the neonatal mouse heart. *Science*. 2011b; 331:1078–1080. [PubMed: 21350179]
- Porrello ER, Widdop RE, Delbridge LM. Early origins of cardiac hypertrophy: does cardiomyocyte attrition programme for pathological 'catch-up' growth of the heart? *Clin Exp Pharmacol Physiol*. 2008; 35:1358–1364. [PubMed: 18759854]
- Poss KD, Wilson LG, Keating MT. Heart regeneration in zebrafish. *Science*. 2002; 298:2188–2190. [PubMed: 12481136]
- Puceat M, Travo P, Quinn MT, Fort P. A dual role of the GTPase Rac in cardiac differentiation of stem cells. *Mol Biol Cell*. 2003; 14:2781–2792. [PubMed: 12857864]
- Quaini F, Urbanek K, Beltrami AP, Finato N, Beltrami CA, Nadal-Ginard B, Kajstura J, Leri A, Anversa P. Chimerism of the transplanted heart. *N Engl J Med*. 2002; 346:5–15. [PubMed: 11777997]
- Rees BB, Sudradjat FA, Love JW. Acclimation to hypoxia increases survival time of zebrafish, *Danio rerio*, during lethal hypoxia. *J Exp Zool*. 2001; 289:266–272. [PubMed: 11241397]
- Reiss K, Cheng W, Ferber A, Kajstura J, Li P, Li B, Olivetti G, Homcy CJ, Baserga R, Anversa P. Overexpression of insulin-like growth factor-1 in the heart is coupled with myocyte proliferation in transgenic mice. *Proc Natl Acad Sci U S A*. 1996; 93:8630–8635. [PubMed: 8710922]
- Reynolds JD, Penning DH, Dexter F, Atkins B, Hrdy J, Poduska D, Brien JF. Ethanol increases uterine blood flow and fetal arterial blood oxygen tension in the near-term pregnant ewe. *Alcohol*. 1996; 13:251–256. [PubMed: 8734839]
- Roesner A, Hankeln T, Burmester T. Hypoxia induces a complex response of globin expression in zebrafish (*Danio rerio*). *J Exp Biol*. 2006; 209:2129–2137. [PubMed: 16709914]
- Rudolph AM, Heyman MA. Fetal and neonatal circulation and respiration. *Annu Rev Physiol*. 1974; 36:187–207. [PubMed: 19400661]
- Santamaria D, Barriere C, Cerqueira A, Hunt S, Tardy C, Newton K, Caceres JF, Dubus P, Malumbres M, Barbacid M. Cdk1 is sufficient to drive the mammalian cell cycle. *Nature*. 2007; 448:811–815. [PubMed: 17700700]
- Sauer H, Rahimi G, Hescheler J, Wartenberg M. Role of reactive oxygen species and phosphatidylinositol 3-kinase in cardiomyocyte differentiation of embryonic stem cells. *FEBS Lett*. 2000; 476:218–223. [PubMed: 10913617]
- Schafer FQ, Buettner GR. Redox environment of the cell as viewed through the redox state of the glutathione disulfide/glutathione couple. *Free Radic Biol Med*. 2001; 30:1191–1212. [PubMed: 11368918]
- Schmelter M, Ateghang B, Helmig S, Wartenberg M, Sauer H. Embryonic stem cells utilize reactive oxygen species as transducers of mechanical strain-induced cardiovascular differentiation. *Faseb J*. 2006; 20:1182–1184. [PubMed: 16636108]
- Schriner SE, Linford NJ, Martin GM, Treuting P, Ogburn CE, Emond M, Coskun PE, Ladiges W, Wolf N, Van Remmen H, et al. Extension of murine life span by overexpression of catalase targeted to mitochondria. *Science*. 2005; 308:1909–1911. [PubMed: 15879174]
- Sdek P, Zhao P, Wang Y, Huang CJ, Ko CY, Butler PC, Weiss JN, MacLellan WR. Rb and p130 control cell cycle gene silencing to maintain the postmitotic phenotype in cardiac myocytes. *J Cell Biol*. 2011; 194:407–423. [PubMed: 21825075]

- Semenza GL. Life with oxygen. *Science*. 2007; 318:62–64. [PubMed: 17916722]
- Sen CK, Rahkila P, Hanninen O. Glutathione metabolism in skeletal muscle derived cells of the L6 line. *Acta Physiol Scand*. 1993; 148:21–26. [PubMed: 8333293]
- Sherr CJ. Cancer cell cycles. *Science*. 1996; 274:1672–1677. [PubMed: 8939849]
- Siggins L, Figg N, Bennett M, Foo R. Nutrient deprivation regulates DNA damage repair in cardiomyocytes via loss of the base-excision repair enzyme OGG1. *FASEB J*. 2012; 26:2117–2124. [PubMed: 22302830]
- Soonpaa MH, Kim KK, Pajak L, Franklin M, Field LJ. Cardiomyocyte DNA synthesis and binucleation during murine development. *Am J Physiol*. 1996; 271:H2183–H2189. [PubMed: 8945939]
- Sundaresan M, Yu ZX, Ferrans VJ, Irani K, Finkel T. Requirement for generation of H₂O₂ for platelet-derived growth factor signal transduction. *Science*. 1995; 270:296–299. [PubMed: 7569979]
- Takahashi A, Ohtani N, Yamakoshi K, Iida S, Tahara H, Nakayama K, Nakayama KI, Ide T, Saya H, Hara E. Mitogenic signalling and the p16INK4a-Rb pathway cooperate to enforce irreversible cellular senescence. *Nat Cell Biol*. 2006; 8:1291–1297. [PubMed: 17028578]
- Tothova Z, Kollipara R, Huntly BJ, Lee BH, Castrillon DH, Cullen DE, McDowell EP, Lazo-Kallanian S, Williams IR, Sears C, et al. FoxOs are critical mediators of hematopoietic stem cell resistance to physiologic oxidative stress. *Cell*. 2007; 128:325–339. [PubMed: 17254970]
- Trachootham D, Alexandre J, Huang P. Targeting cancer cells by ROS-mediated mechanisms: a radical therapeutic approach? *Nat Rev Drug Discov*. 2009; 8:579–591. [PubMed: 19478820]
- Tsatmali M, Walcott EC, Makarenkova H, Crossin KL. Reactive oxygen species modulate the differentiation of neurons in clonal cortical cultures. *Mol Cell Neurosci*. 2006; 33:345–357. [PubMed: 17000118]
- Turrens JF. Superoxide production by the mitochondrial respiratory chain. *Biosci Rep*. 1997; 17:3–8. [PubMed: 9171915]
- Turrens JF. Mitochondrial formation of reactive oxygen species. *J Physiol*. 2003; 552:335–344. [PubMed: 14561818]
- Wang J, Panakova D, Kikuchi K, Holdway JE, Gemberling M, Burris JS, Singh SP, Dickson AL, Lin YF, Sabeh MK, et al. The regenerative capacity of zebrafish reverses cardiac failure caused by genetic cardiomyocyte depletion. *Development*. 2011; 138:3421–3430. [PubMed: 21752928]
- Webster WS, Abela D. The effect of hypoxia in development. *Birth Defects Res C Embryo Today*. 2007; 81:215–228. [PubMed: 17963271]
- Werner JC, Sicard RE. Lactate metabolism of isolated, perfused fetal, and newborn pig hearts. *Pediatr Res*. 1987; 22:552–556. [PubMed: 3684382]
- Wisneski JA, Gertz EW, Neese RA, Gruenke LD, Morris DL, Craig JC. Metabolic fate of extracted glucose in normal human myocardium. *J Clin Invest*. 1985; 76:1819–1827. [PubMed: 4056055]
- Xin M, Kim Y, Sutherland LB, Murakami M, Qi X, McAnally J, Porrello ER, Mahmoud AI, Tan W, Shelton JM, et al. Hippo pathway effector Yap promotes cardiac regeneration. *Proc Natl Acad Sci U S A*. 2013; 110:13839–13844. [PubMed: 23918388]
- Yoneyama M, Kawada K, Gotoh Y, Shiba T, Ogita K. Endogenous reactive oxygen species are essential for proliferation of neural stem/progenitor cells. *Neurochem Int*. 2010; 56:740–746. [PubMed: 19958807]
- Zhao H, Joseph J, Fales HM, Sokoloski EA, Levine RL, Vasquez-Vivar J, Kalyanaraman B. Detection and characterization of the product of hydroethidine and intracellular superoxide by HPLC and limitations of fluorescence. *Proc Natl Acad Sci U S A*. 2005; 102:5727–5732. [PubMed: 15824309]

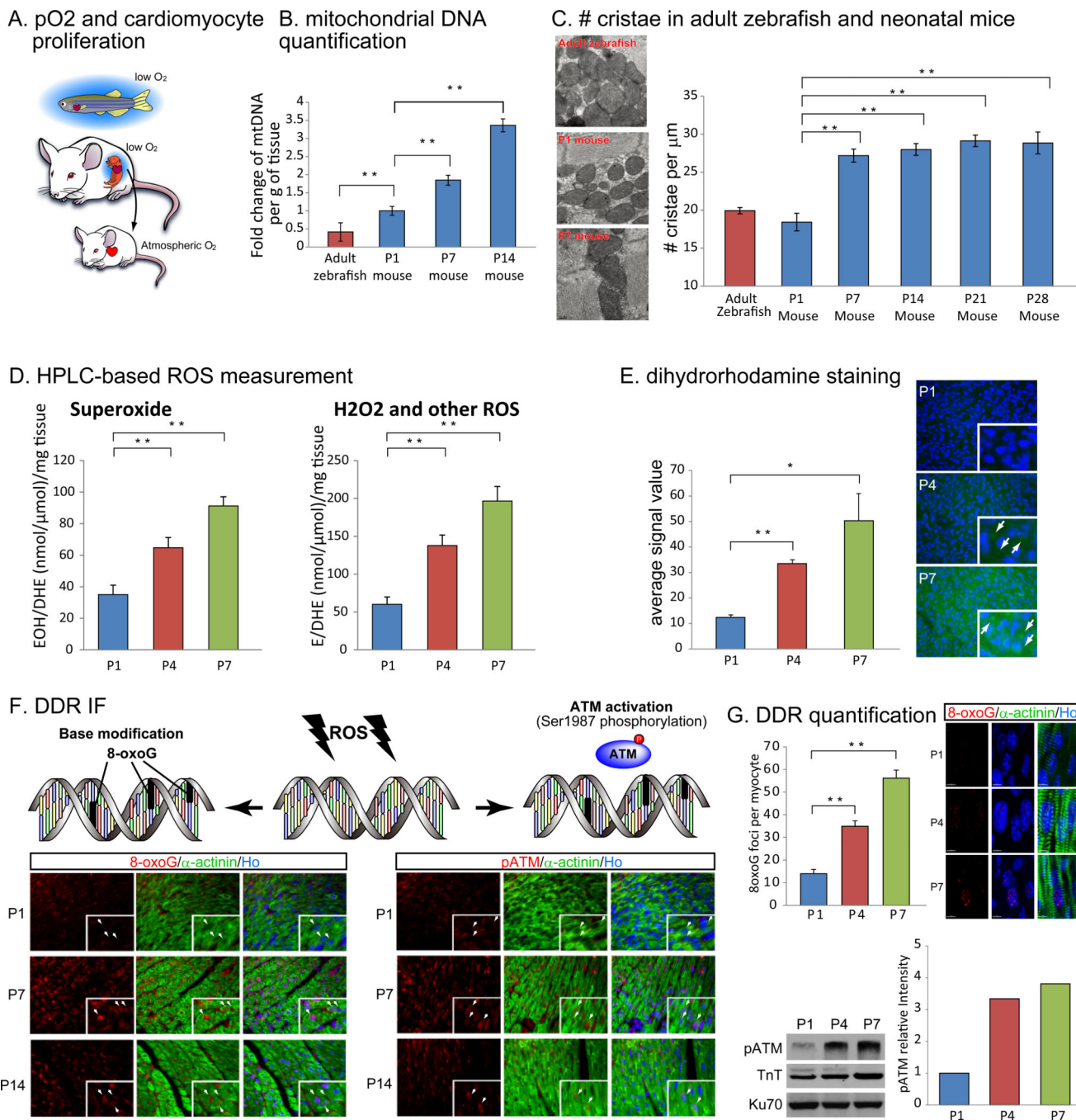


Figure 1. Oxidation state, activity of mitochondrial respiration, oxidative stress and the activation of DNA damage response (DDR) correspond to cardiac regenerative capacity. (A) Fishes and mammalian fetuses are under low-oxygenated environment, whereas postnatal mammals are in well-oxygenated atmosphere. (B) qPCR analysis revealed post-natal increase in mitochondrial DNA (mtDNA) contents per gram of tissue (ventricles) until postnatal day 14 (P14). Relative mtDNA content in adult zebrafish was even smaller than that in P1 mouse. (C) TEM images of ventricles showed more mature cristae structure in P7 mouse heart

comparing with P1 mouse heart and adult zebrafish heart (left). The number of mitochondrial cristae counted from SEM images increased in P7 mouse heart compared to P1 mouse heart (table, blue bars) and also to adult zebrafish heart (table, red bar). (D) HPLC detection of a superoxide probe dihydroethidium (DHE) revealed a significant increase in both 2-hydroxyethidium (EOH), a specific product for superoxide anion radical, and in ethidium (E), oxidized by other reactive oxygen species such as H_2O_2 (mainly) and ONOO from P1 to P7. (E) Imaging of ROS on cryosections with dihydrorhodamine 123 staining indicated linear increase in cardiomyocyte ROS level from P1 to P7 (arrows). (F) Immunostaining with oxidative DNA damage and DDR markers. A marker for oxidative base modification in DNA, 8-oxo-7,8-dihydroguanine (8-oxoG, left panels), and for activation of DDR, Ser1987 phosphorylated ATM (pATM, right panels) were not detected in cardiomyocyte nuclei at P1 (top panels, white arrows), whereas at P7 (middle panels) and at P14 (lower panels) both 8-oxoG and pATM showed nuclear localization (co-localized with Hoechst 33258, Ho) indicated by arrows. (G) Oxidative DNA damage and DDR were induced before P7 in cardiomyocyte. Left panels show representative images of 3D imaging of 8-oxoG staining and the number of 8-oxoG foci per cardiomyocyte. Right panels show western blot and quantification of pATM indicating upregulation of DDR. Cardiac troponin T (TnT) was used to normalize sample loading. Error bars indicate SEM. * $p < 0.05$; ** $p < 0.01$.

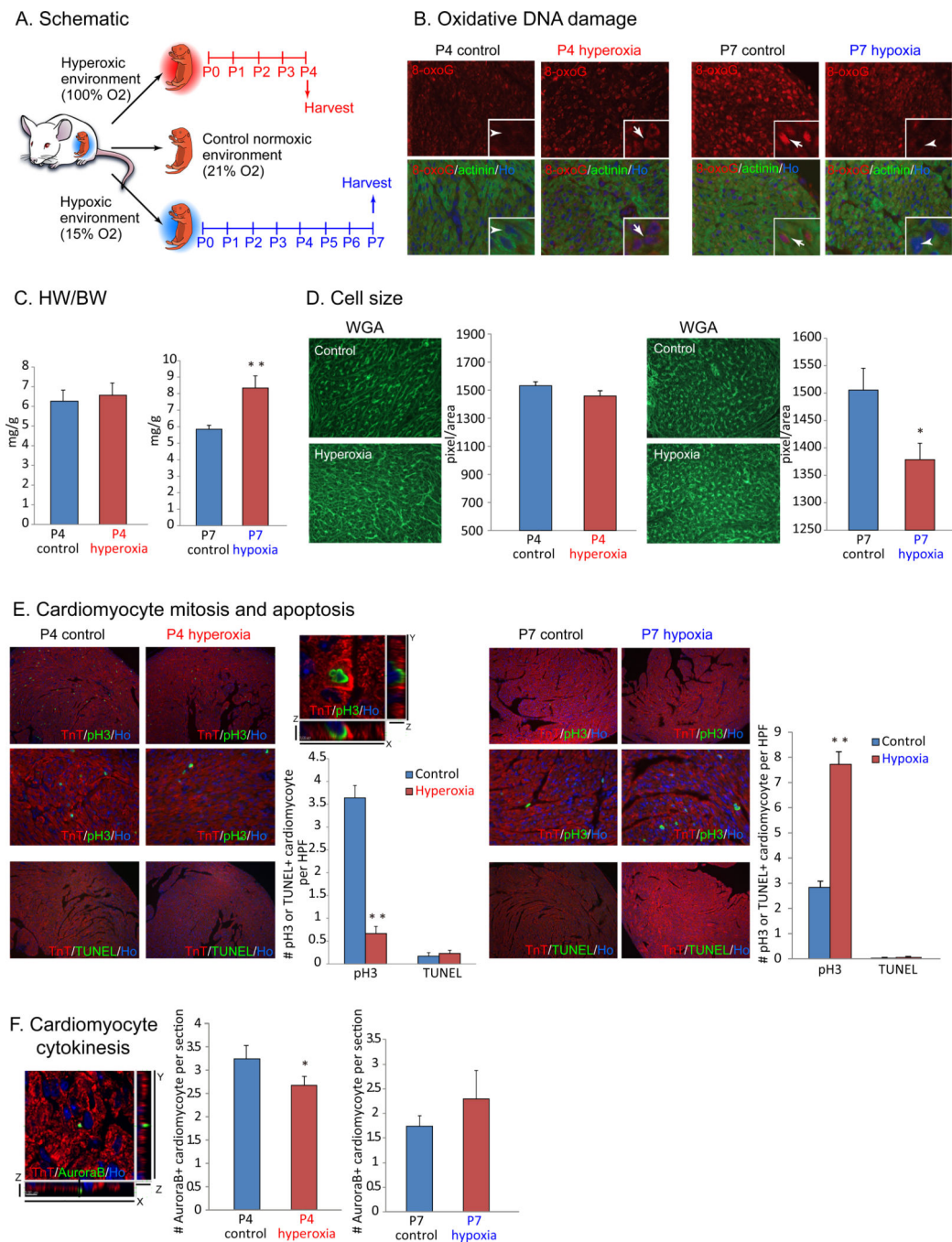


Figure 2. Postnatal cardiomyocyte cell cycle arrest is dependent on environmental oxygen concentration. (A) Neonates were exposed to hyperoxic (100% O₂) or mildly hypoxic (15% O₂) environment from perinatal stage for 4 days (hyperoxia) or 7 days (hypoxia). (B) Oxidative DNA damage indicated by nuclear signal with anti-8-oxoG antibody in cardiomyocyte was increased in hyperoxic hearts (left panels), and decreased in hypoxic hearts (right panels). (C) Heart weight versus body weight (HW/BW) ratio showed no statistically significant difference in mice exposed to hyperoxia, whereas significantly

increased in mice exposed to hypoxia. (D) Cardiomyocyte cell size did not show significant difference in hyperoxia, and was decreased in hypoxia. (E) Co-immunostaining with anti-phospho-histone H3 Ser10 (pH3) and anti-cardiac Troponin T (TnT) antibodies showed drastic decrease in cardiomyocyte mitosis in hyperoxia-exposed hearts, and in contrast, significant increase in cardiomyocyte mitosis in hypoxia-exposed hearts. Cardiomyocyte apoptosis did not increase in neither treatments as shown by TUNEL staining. (F) Co-immunostaining with anti-Aurora B and anti-sarcomeric actinin antibodies showed decreased cytokinesis in hyperoxic hearts, whereas mild increase in hypoxic hearts. Error bars indicate SEM. * $p < 0.05$; ** $p < 0.01$.

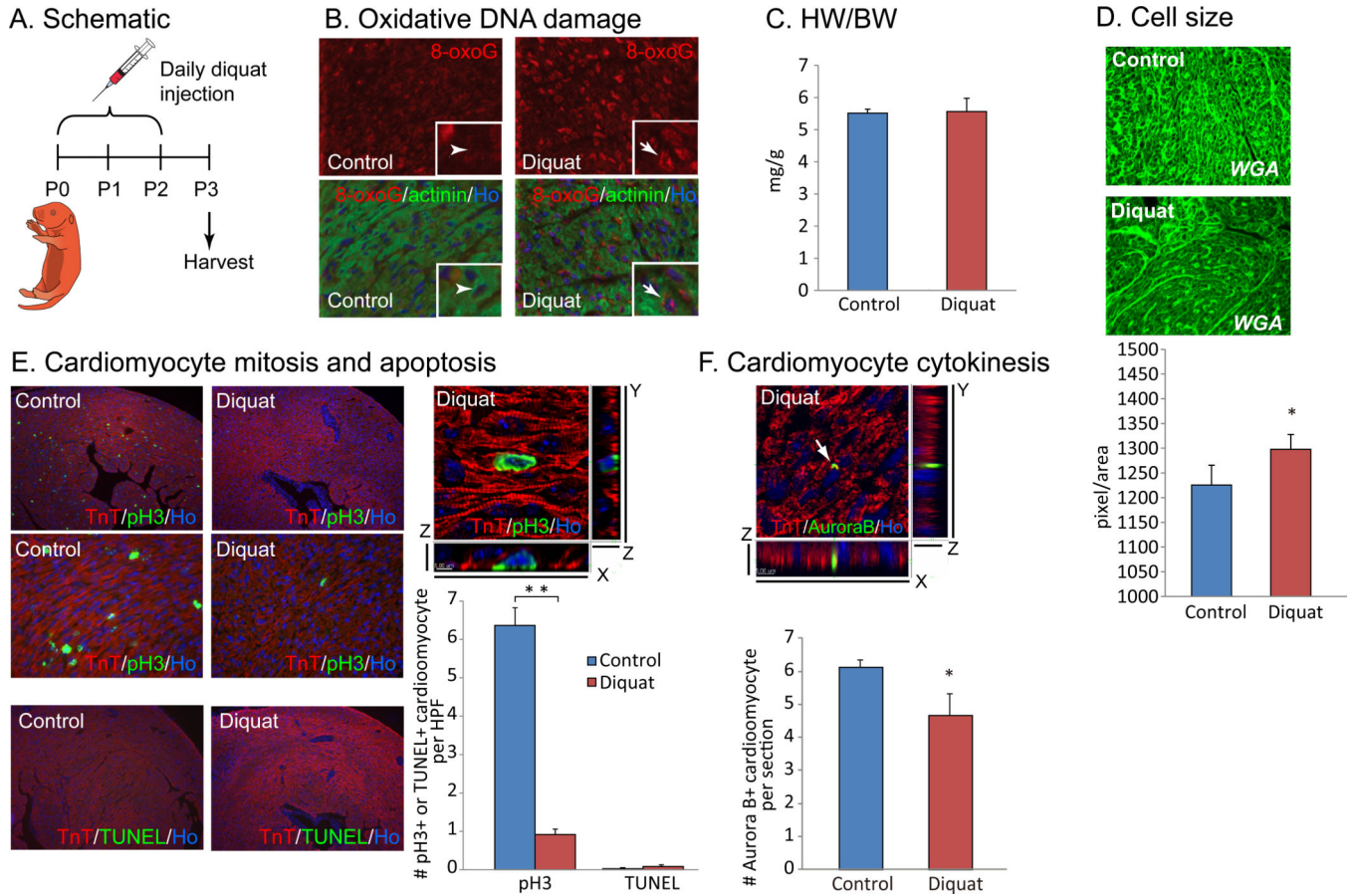


Figure 3. Injection of ROS generator diquat induced accelerated cardiomyocyte cell cycle arrest. (A) 5mg/kg of diquat was injected subcutaneously for 3 days after birth and hearts were harvested at P3. (B) Immunostaining showed nuclear accumulation of 8-oxoG in cardiomyocytes in diquat injected neonates. (C) HW/BW ratio has no statistically significant difference. (D) WGA staining showed significantly increased cardiomyocyte cell size in hearts of diquat injected neonates. (E) Co-immunostaining with anti-pH3 and anti-TnT antibodies showed drastic decrease in cardiomyocyte mitosis in diquat injected hearts. TUNEL assay showed no significant increase in cardiomyocyte apoptosis. (F) Diquat injection resulted in decreased cardiomyocyte cytokinesis as shown by co-immunostaining with anti-Aurora B, anti-TnT antibodies. Error bars indicate SEM. * $p < 0.05$; ** $p < 0.01$.

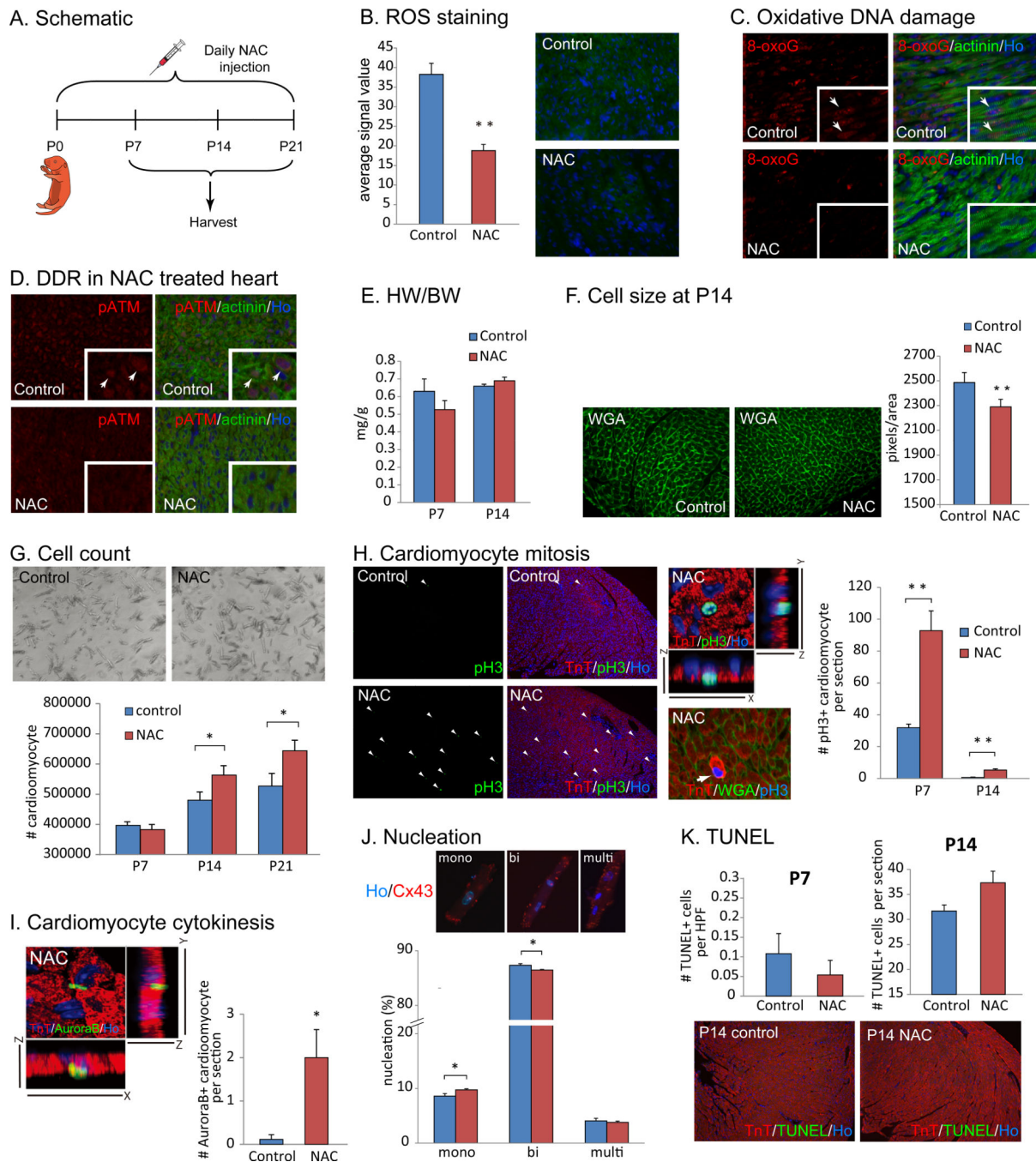


Figure 4. Injection of a scavenger against ROS suppresses post-natal cardiomyocyte cell cycle arrest. (A) N-acetyl-cysteine (NAC) was administered for 21 days after birth. (B) ROS level in cardiomyocytes significantly decreased as shown by dihydrorhodamine 123 staining in NAC treated neonates. (C) Reduced 8-oxoG staining was seen in NAC injected heart, demonstrating reduced oxidative DNA damage in cardiomyocyte at P7. (D) NAC injection suppressed activation of DNA damage response pathway. Co-immunostaining with anti-pATM and anti-alpha actinin antibodies showed that NAC treatment reduces nuclear

phospho-ATM at P7 compared with control (arrows in left panels). (E) HW/BW ratio in control and NAC treated hearts at P14 showed no significant difference. (F) Cell size quantification using WGA staining showed significantly decreased cell size in NAC treated hearts. (G) Total number of cardiomyocyte was significantly increased in NAC treated heart at P21. (H) Co-immunostaining with anti-pH3 and anti-TnT antibodies showed increased cardiomyocyte mitosis in NAC treated hearts. Images shown are hearts from PBS-injected control or NAC-injected neonates at P14. (I) NAC injection induced cardiomyocyte cytokinesis indicated by Aurora B and TnT double positive cardiomyocytes. (J) Percentage of binucleated cardiomyocytes was significantly decreased and mononucleation was significantly increased in NAC treated hearts at P14. Immunocytochemistry on isolated myocyte with anti-Cx43 antibody and Hoechst 33258 (Ho) nuclear specific dye were used to visualize boundary and nuclei of each cardiomyocyte, respectively. (K) Apoptotic cell death visualized with TUNEL assay was not increased in NAC-treated heart at neither P7 nor P14. Error bars indicate SEM. * $p < 0.05$; ** $p < 0.01$.

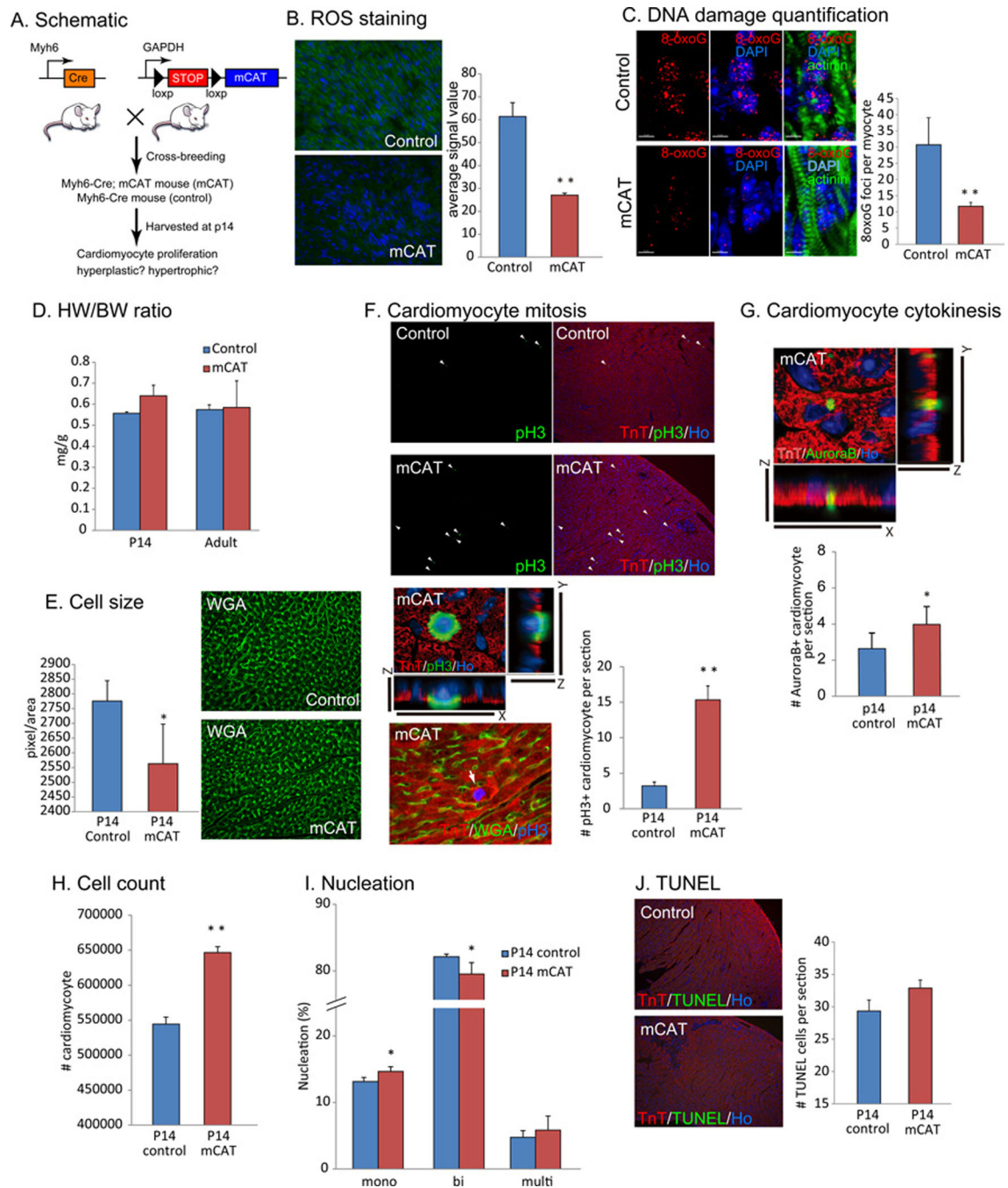


Figure 5. Scavenging reactive oxygen species in mitochondria suppresses post-natal cardiomyocyte cell cycle arrest. (A) Mitochondrial-targeted catalase (mCAT) was over-expressed in cardiomyocyte by flipping floxed-stop cassette between GAPDH promoter and mCAT by crossing with mice harboring Myh6 promoter driven Cre recombinase. Myh6-Cre; floxed-stop mCAT mice are hereinafter called mCAT mice. Litter-mate Myh6-Cre mice were used as control. (B) The level of ROS in cardiomyocyte decreased in mCAT heart compared with control. (C) mCAT significantly suppressed DNA damage shown by 3D imaging and the

quantification of 8-oxoG foci in cardiomyocyte (D) HW/BW ratio in control and mCAT mouse hearts at P14 and in the adult was not changed. (F) WGA staining indicated slightly decreased cardiomyocyte cell size in mCAT mouse heart, but not statistically significant level. (G) Increased cardiomyocyte mitosis in mCAT mouse hearts at p14 indicated by co-immunostaining with anti-pH3 and anti-troponin T antibodies. (H) Increase in cardiomyocyte cytokinesis shown by immunostaining with anti-Aurora B antibody. (I) Total number of cardiomyocyte was significantly increased at P14 in mCAT mouse heart. (J) Number of binucleated cardiomyocytes was significantly decreased and mononucleated cardiomyocytes was significantly increased in mCAT hearts (K) TUNEL positive apoptotic cell death was within normal range in mCAT heart. Error bars indicate SEM. * $p < 0.05$; ** $p < 0.01$.

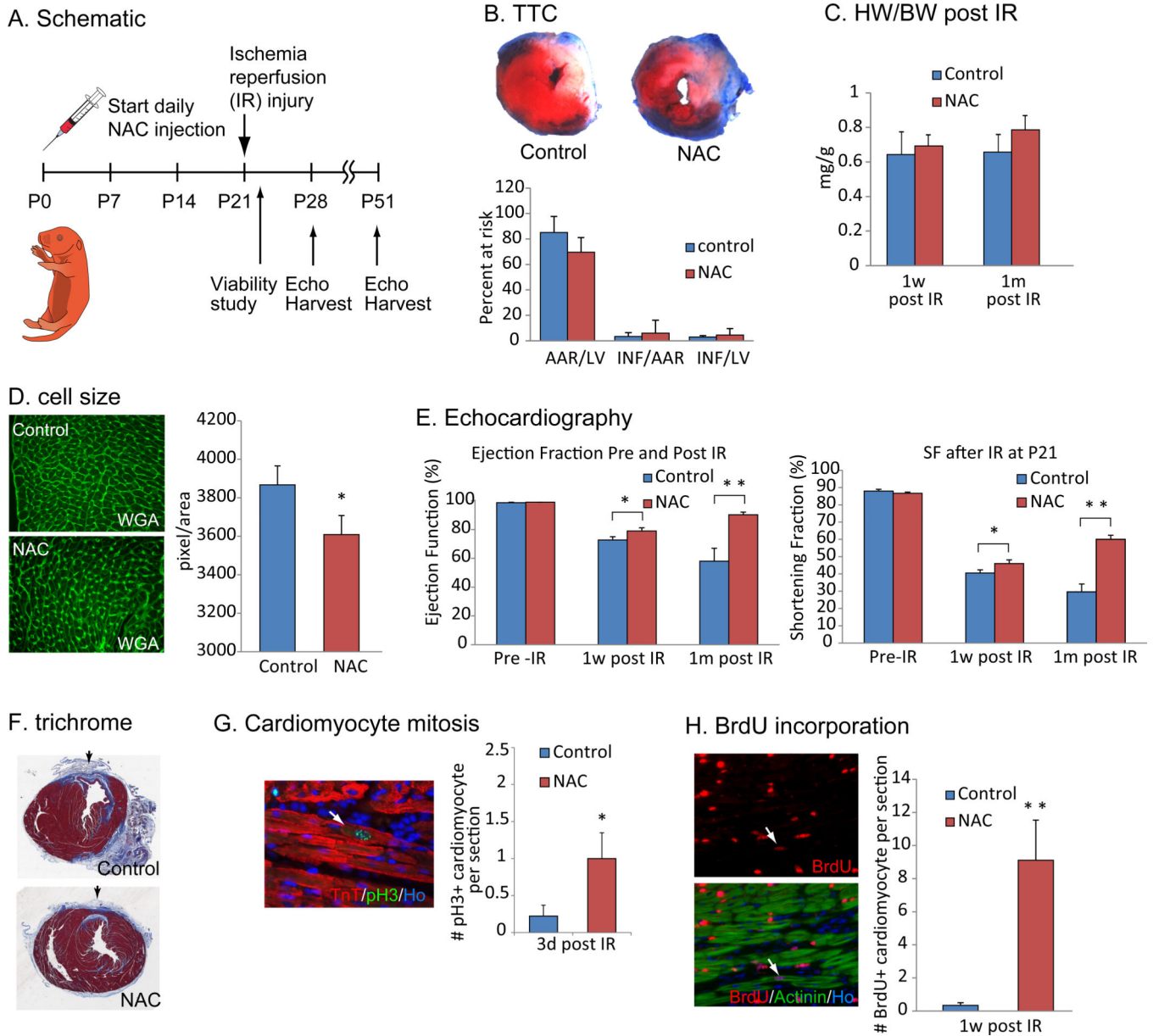


Figure 6. Scavenging ROS extends postnatal cardiac regeneration window. (A) Animals were treated with NAC from P0 and subjected to ischemia reperfusion (IR) surgery at P21. Viability was investigated 24 hours after injury to evaluate the consistency of the IR surgery, and then cardiac function was examined by echocardiography at 1 week and 1 month after injury. (B) TTC staining showed no significant difference in the size of injury between control and NAC-pretreated hearts. (C) HW/BW ratio at 1 week or 1 month after IR surgery between control and NAC-pretreated mice was not changed. (D) WGA staining showed a decrease in cell size in NAC treated hearts 1 month after IR injury compared to control hearts, indicating the NAC treatment did not induce cardiomyocyte hypertrophy. (E) Left ventricular systolic function quantified by ejection fraction (EF) and shortening fraction (SF) (n=6 per group) before IR surgery (left), 1 week after surgery (middle) and 1 month after

surgery (right) showed more functional recovery in NAC-pretreated hearts compared with control hearts. (F) Histological analysis with Masson trichrome staining showed reduced fibrotic scar formation in NAC treated hearts. (G) Cardiomyocyte mitosis was increased in NAC-treated mice as indicated by anti-pH3 and anti-TnT co-immunostaining at 3 days after IR injury. (H) Immunostaining with anti-BrdU and anti-Actinin antibodies showed increased cardiomyocyte BrdU incorporation NAC-pretreated heart. Error bars indicate SEM. * $p < 0.05$; ** $p < 0.01$.

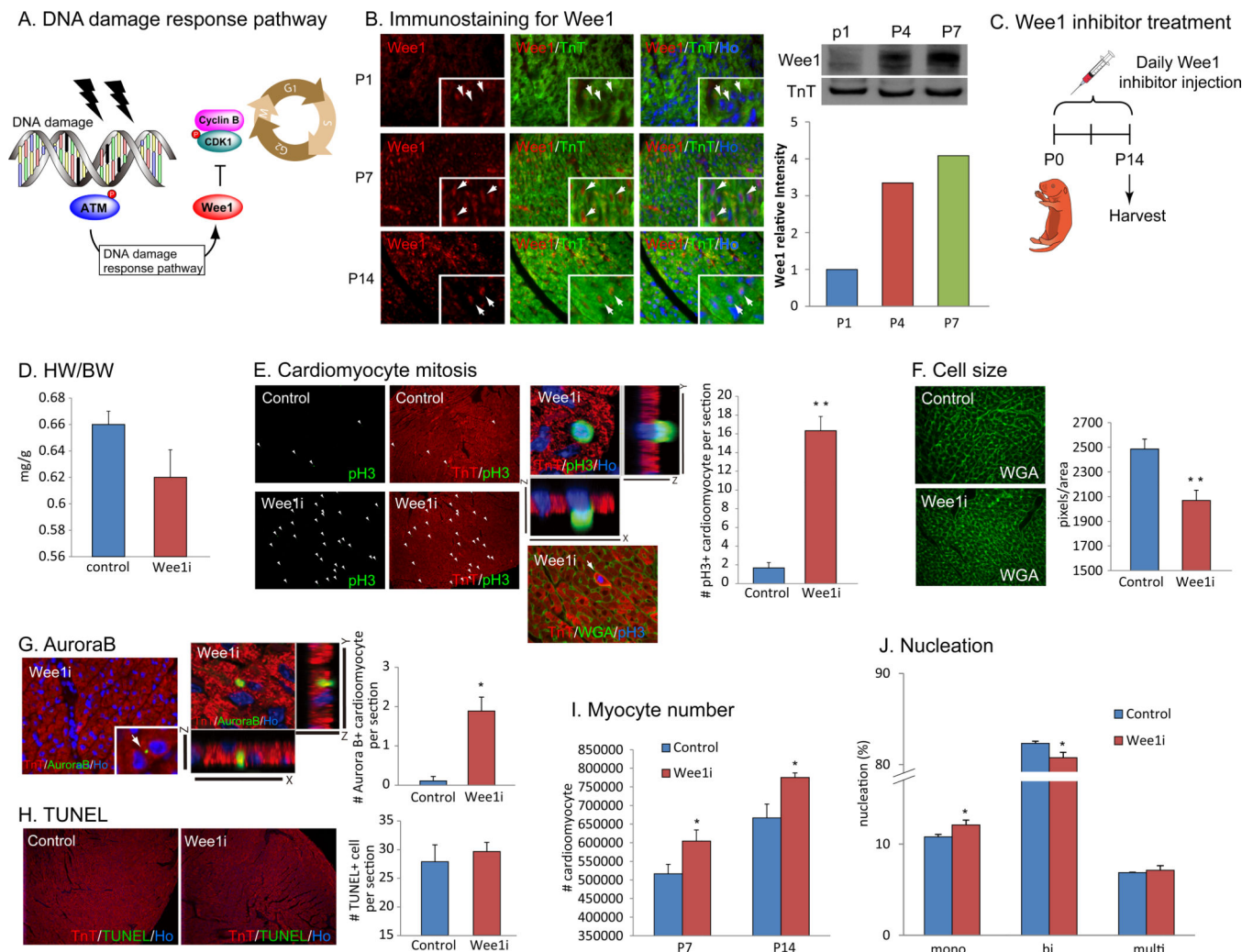


Figure 7. Inhibition of an effector of DNA damage response, Wee1 kinase, suppresses postnatal cardiomyocyte cell cycle arrest. (A) DNA damage response pathway activates Wee1 kinase that inhibits cell cycle regulator Cyclin/CDKs, resulting in cell cycle arrest. (B) Immunostaining with anti-Wee1 and anti-TnT antibodies showed no expression of Wee1 protein in cardiomyocytes at P1 (arrows), and then nuclear localized Wee1 protein at P7 and P14 (arrows). (C) Daily injection of Wee1 kinase inhibitor MK-1775 was performed from birth until P14. (D) Wee1 inhibitor injection resulted in slight, but not statistically significant, decrease in HW/BW ratio compared with control. (E) Inhibition of Wee1 induced mitosis in cardiomyocyte at P14 shown by pH3/TnT immunostaining. (F) Quantification of cardiomyocyte cell size with WGA staining showed decreased cardiomyocyte size in Wee1 inhibitor treated hearts. (G) AuroraB/TnT immunostaining showed increased cardiomyocyte cytokinesis in Wee1 inhibitor treated hearts. (H) No increase in apoptotic cell death in cardiomyocyte indicated by TUNEL assay. (I) Total number of cardiomyocyte was increased at P7 and P14 in Wee1 inhibitor treated hearts. (J) Number of binucleated cardiomyocytes was reduced, and mononucleated cardiomyocyte

was increased in Wee1 inhibitor treated heart. Error bars indicate SEM. * $p < 0.05$; ** $p < 0.01$.